HEALTH AND MEDICINE

Editing a γ-globin repressor binding site restores fetal hemoglobin synthesis and corrects the sickle cell disease phenotype

Leslie Weber[1,2,3]*, Giacomo Frati[3,4]*, Tristan Felix[3,4], Giulia Hardouin[3,4], Antonio Casini[5], Clara Wollenschlaeger[3,4], Vasco Meneghini[3,4], Cecile Masson[6], Anne De Cian[7], Anne Chalumeau[1,3,4], Fulvio Mavilio[8,9], Mario Amendola[10], Isabelle Andre-Schmutz[1,4], Anna Cereseto[5], Wassim El Nemer[11,12,13], Jean-Paul Concordet[7], Carine Giovannangeli[7], Marina Cavazzana[1,4,14], Annarita Miccio[3,4†]

Sickle cell disease (SCD) is caused by a single amino acid change in the adult hemoglobin (Hb) β chain that causes Hb polymerization and red blood cell (RBC) sickling. The co-inheritance of mutations causing fetal γ-globin production in adult life hereditary persistence of fetal Hb (HPFH) reduces the clinical severity of SCD. HPFH mutations in the *HBG* γ-globin promoters disrupt binding sites for the repressors BCL11A and LRF. We used CRISPR-Cas9 to mimic HPFH mutations in the *HBG* promoters by generating insertions and deletions, leading to disruption of known and putative repressor binding sites. Editing of the LRF-binding site in patient-derived hematopoietic stem/progenitor cells (HSPCs) resulted in γ-globin derepression and correction of the sickling phenotype. Xenotransplantation of HSPCs treated with gRNAs targeting the LRF-binding site showed a high editing efficiency in repopulating HSPCs. This study identifies the LRF-binding site as a potent target for genome-editing treatment of SCD.

INTRODUCTION

β-Hemoglobinopathies (SCD and β-thalassemia) are severe anemias characterized by abnormal or reduced production of hemoglobin (Hb) β chains. SCD and β-thalassemia are the most common monogenic disorders with an incidence of 1 per 318,000 live births worldwide. In β-thalassemia, the reduced production of β chains causes α-globin precipitation and insufficiently hemoglobinized red blood cells (RBCs). In SCD, the $\beta 6^{Glu \rightarrow Val}$ substitution leads to Hb polymerization and RBC sickling, which is responsible for vaso-occlusive crises, hemolytic anemia, and organ damage.

Allogeneic hematopoietic stem cell (HSC) transplantation is the only definitive cure for patients affected by SCD or β-thalassemia. Transplantation of autologous, genetically modified HSCs represents a promising therapeutic option for patient lacking a compatible HSC donor (*1*). Pioneering clinical trials based on lentiviral (LV)–based gene addition approaches demonstrated a clinical benefit in β-thalassemic patients with residual β-globin production (β^+-thalassemia). However, this treatment is, at best, partially effective in correcting the clinical phenotype of severe β^0-thalassemia (no residual β-globin production) and SCD patients, where higher levels of therapeutic globin are required to restore correct globin chain balance and inhibit HbS polymerization (*2*–*6*).

The clinical severity of β-hemoglobinopathies is alleviated by the co-inheritance of genetic mutations causing a sustained fetal γ-globin chain production at adult age, a condition termed hereditary persistence of fetal Hb (HPFH) (*7*). Elevated fetal γ-globin levels reduce globin chain imbalance in β-thalassemias and exert a potent anti-sickling effect in SCD. Compared with current LV-based gene addition approaches, therapeutic strategies aimed at forcing a β-globin–to–γ-globin switch (*8*) have the advantage of guaranteeing high-level expression of the endogenous γ-globin genes and, in the case of SCD, reduction of the β^S-globin synthesis.

HPFH mutations and single-nucleotide polymorphisms (SNPs) associated with HbF levels of up to 40% of the total Hb were identified at positions −200, −175, −158, and −115 upstream of the *HBG1* and *HBG2* transcription start sites (TSSs) (Fig. 1A). These mutations either generate de novo DNA motifs recognized by transcriptional activators (*9*, *10*) or disrupt the binding sites for transcriptional repressors. In particular, HPFH mutations in the −200 and −115 regions reduce the binding of LRF and BCL11A transcriptional repressors, respectively, thus inhibiting γ-globin silencing (*11*, *12*). In addition, SNPs at position −158 of both *HBG* γ-globin promoters are associated with enhanced γ-globin expression (*13*–*17*). These SNPs might either identify a putative transcriptional repressor binding site or create a binding site for a transcriptional activator. An ideal and universal strategy to correct the clinical phenotype of patients with β-hemoglobinopathies would be to introduce HPFH mutations in the γ-globin promoters via homology-directed repair (*11*), which, however, is inefficient in HSCs (*18*). Here, we mimicked HPFH mutations by disrupting known or putative binding sites for transcriptional repressors in the γ-globin promoters using a CRISPR-Cas9–based genome editing strategy that takes advantage of the nonhomologous

[1]Laboratory of Human Lymphohematopoiesis, INSERM UMR1163, Paris, France. [2]Paris Diderot University–Sorbonne Paris Cité, Paris, France. [3]Laboratory of chromatin and gene regulation during development, INSERM UMR1163, Paris, France. [4]Paris Descartes–Sorbonne Paris Cité University, Imagine Institute, Paris, France. [5]CIBIO, University of Trento, Trento, Italy. [6]Paris-Descartes Bioinformatics Platform, Imagine Institute, Paris 75015, France. [7]INSERM U1154, CNRS UMR7196, Museum National d'Histoire Naturelle, Paris, France. [8]Department of Life Sciences, University of Modena and Reggio Emilia, Modena, Italy. [9]Audentes Therapeutics, San Francisco, CA, USA. [10]Genethon, INSERM UMR951, Evry, France. [11]Biologie Intégrée du Globule Rouge UMR_S1134, Inserm, Univ. Paris Diderot, Sorbonne Paris Cité, Univ. de la Réunion, Univ. des Antilles, Paris, France. [12]Institut National de la Transfusion Sanguine, F-75015 Paris, France. [13]Laboratoire d'Excellence GR-Ex, Paris, France. [14]Biotherapy Department, Necker Children's Hospital, Assistance Publique–Hôpitaux de Paris, Paris, France.
*These authors contributed equally to this work as co-first authors.
†Corresponding author. Email: annarita.miccio@institutimagine.org

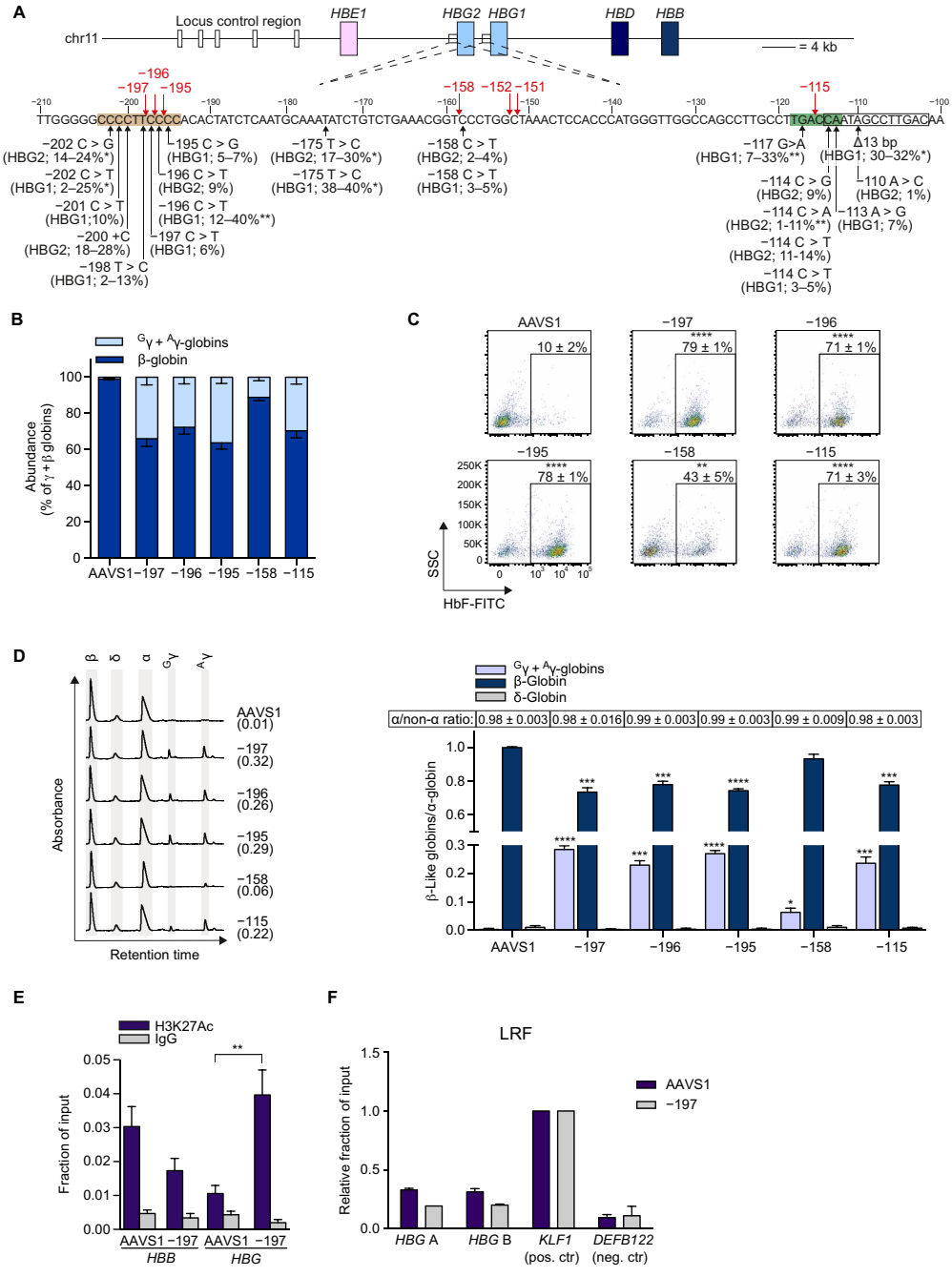

Fig. 1. LRF-binding site disruption induces γ-globin expression in HUDEP-2 cells. (**A**) Schematic representation of the β-globin locus on chromosome 11, depicting the hypersensitive sites of the locus control region (white boxes) and the *HBE1*, *HBG2*, *HBG1*, *HBD*, and *HBB* genes (colored boxes). The sequence of the *HBG2* and *HBG1* identical promoters (from −210 to −100 nucleotides upstream of the *HBG* TSS) is shown below. Black arrows indicate HPFH mutations described at *HBG1* and/or *HBG2* promoters, with the percentage of HbF in heterozygous carriers of HPFH mutations (*42*). The highest HbF levels were generally observed in individuals carrying SCD (*) or β-thalassemia mutations (**). LRF- and BCL11A-binding sites [as described in (*11*)] are highlighted by orange and green boxes, respectively. The −114/−102 13-bp HPFH deletion is indicated by an empty box. Red arrows indicate the gRNA cleavage sites. (**B** to **E**) Globin expression analyses were performed in mature erythroblasts differentiated from Cas9-GFP$^+$ HUDEP-2 cells. Results are shown as means ± SEM of three to four independent experiments. (B) RT-qPCR quantification of (^{G}γ + ^{A}γ)- and β-globin transcripts. mRNA levels were expressed as percentage of (γ + β) globins, after normalization to α-globin mRNA levels. (C) Representative flow cytometry plots showing the percentage of HbF$^+$ cells. (D) RP-HPLC analysis of globin chains. β-Like globin expression was normalized to α-globin. Representative RP-HPLC chromatograms are reported together with the expression of γ-globin chains (in brackets). The ratio of α chains to non–α chains was similar between *HBG*-edited and control samples. (E) ChIP-qPCR analysis of H3K27Ac at *HBB* and *HBG* promoters in −197-edited HUDEP-2 cells and control *AAVS1*–edited samples (day 5 of differentiation, $n = 3$). ChIP was performed using an antibody against H3K27Ac and the corresponding control immunoglobulin G (IgG). ****$P \leq 0.0001$, ***$P \leq 0.001$, **$P \leq 0.01$, and *$P \leq 0.05$ (unpaired t test). SSC, side scatter. (**F**) ChIP-qPCR analysis of LRF at *HBG* promoters in −197-edited and control *AAVS1*–edited K562 cells ($n = 2$ biologically independent experiments). ChIP was performed using an antibody against LRF. Two different primer pairs were used to amplify the *HBG* promoters (A and B). *KLF1* and *DEFB122* served as positive and negative controls, respectively.

end joining (NHEJ)– and microhomology (MH)–mediated end joining (MMEJ)–mediated DNA repair mechanisms to induce insertions and deletions (InDels) within the γ-globin repressor DNA binding motifs. In particular, we show that efficient disruption of known (−200) or putative (−158) binding sites via CRISPR-Cas9 leads to HbF derepression and thus mimics the effect of HPFH mutations and SNPs in erythroid cell lines and in RBCs derived from SCD patients' hematopoietic stem/progenitor cells (HSPCs). Targeting the LRF-binding site corrects the SCD cell phenotype and is effective in repopulating HSPCs.

RESULTS

Targeting multiple regions in the *HBG* promoters induces HbF expression in adult HUDEP-2 erythroid cells

We designed guide RNAs (gRNAs) targeting the −200 LRF-binding site (−197, −196, and −195) and the −158 region (−158, −152, and −151) (Fig. 1A). In parallel, we used a gRNA targeting the −115 region (−115) that was reported to induce HbF reactivation by generating a 13–base pair (bp) deletion spanning the BCL11A-binding site (*19*) and a control gRNA targeting the unrelated *AAVS1* locus. Plasmid delivery of individual gRNAs and a Cas9–green fluorescent protein (GFP) fusion in the erythroleukemia cell line K562 revealed a similar editing efficiency for the gRNAs targeting the −200 region, whereas the −158 gRNA showed the highest editing efficiency at the −158 region. High cleavage efficiency was also observed for the −115 and *AAVS1* gRNAs (fig. S1A).

We next used the HUDEP-2 adult erythroid cell line to evaluate γ-globin derepression following disruption of the −200, −158, and −115 regions. After plasmid transfection, bulk populations of Cas9-GFP$^+$ HUDEP-2 cells were differentiated into mature erythroblasts. Overall, genome editing efficiency was ~80% for all the gRNAs tested, with the exception of the −158 gRNA (50 ± 4%; fig. S1B). The editing frequency was similar at days 0 and 9 of erythroid differentiation, thus showing that edited cells were not counterselected during erythroid maturation (fig. S1B). The presence of a −158 C>T heterozygous SNP in the *HBG2* promoter resulted in a reduced editing of *HBG2* compared to *HBG1* with the gRNA −158 (40 ± 6% versus 68 ± 1%; fig. S1C). Similar editing frequencies at the *HBG1* and *HBG2* promoters were observed with the other gRNAs (fig. S1C). Deep sequencing analysis revealed that virtually all the editing events altered the LRF- and BCL11A-binding sites in −200 and −115 edited samples, respectively, mostly through small deletions (fig. S1D). In a fraction of β-globin loci, simultaneous cleavage of the *HBG* promoters resulted in the deletion of the intervening 4.9-kb genomic region and loss of the *HBG2* gene, with a frequency ranging from 9 ± 1% to 16 ± 3% (fig. S1E).

Editing of the *HBG* promoters did not alter erythroid cell differentiation, as assessed by morphological analysis, and flow cytometry and reverse transcription quantitative polymerase chain reaction (RT-qPCR) analysis of erythroid markers (fig. S2, A to C). Disruption of the −200 region increased the production of γ-globin transcripts and a parallel decrease of adult β-globin and δ-globin mRNA synthesis (Fig. 1B and fig. S2D). Similar changes were observed upon targeting the −115 region, while a lower γ-globin reactivation was observed upon targeting the −158 region (Fig. 1B and fig. S2D). ε-Globin mRNA levels were not significantly different among *HBG*-edited and control samples (fig. S2D). Flow cytometric analysis of cells edited at −197, −196, and −195 positions revealed a high frequency of HbF-expressing cells (F cells) (79 ± 1%, 71 ± 1%, and 78 ± 1%). Similar results were obtained by disrupting the −115 region (71 ± 3%), while a lower percentage of F cells (43 ± 5%) was obtained in the −158 edited samples (Fig. 1C). Reversed-phase high-performance liquid chromatography (RP-HPLC) confirmed the significant increase in γ-globin with concomitant decrease of β-globin production following editing of the −200 and the −115 regions, while −158 edited cells displayed a milder increase in γ-globin levels (Fig. 1D). Targeting the LRF-binding site resulted in high HbF levels, accounting for up to 28 ± 1% of the total Hb in −197 samples, as determined by cation-exchange HPLC (CE-HPLC). Cells edited with the −115 gRNA showed comparable HbF reactivation (24 ± 3%), while −158 edited cells showed HbF levels of only 5 ± 2% (fig. S2E). HbF mainly contained $^{A}\gamma$ (HBG1) rather than $^{G}\gamma$ (HBG2) chains, which could be explained by loss of *HBG2* caused by the 4.9-kb deletion (fig. S2F). Moreover, cells carrying the 4.9-kb deletion may reactivate more potently γ-globin expression, as the *HBG1-HBG2* intervening sequence might contain cis regulatory elements that repress *HBG* transcription. *HBG*-edited HUDEP-2 showed a normal α chain/non–α chain ratio, indicating that the increased production of γ-globin chains compensated for the reduction of β-globin synthesis (Fig. 1D).

Disruption of the LRF-binding site at both *HBG* promoters was associated with increased H3K27 acetylation (H3K27Ac), a marker of active regulatory elements (Fig. 1E). Concomitantly, H3K27Ac tended to be reduced at the *HBB* gene in −197 edited cells compared to control samples (Fig. 1E). As LRF binding cannot be detected at the *HBG* promoters in wild-type HUDEP-2 cells expressing low HbF levels (*11*), we evaluated LRF binding in HbF$^+$ K562 edited using the −197 gRNA (66% of editing efficiency) or the AAVS1 control gRNA (72% of editing efficiency). Chromatin immunoprecipitation (ChIP)–qPCR experiments showed a twofold reduction in LRF binding in −200-edited cells.

Efficient editing of the *HBG* promoters in SCD HSPCs

To test the anti-sickling properties of induced γ-globin synthesis in a clinically relevant model, we edited the γ-globin repressor binding sites in CD34$^+$ HSPCs obtained from SCD patients by plerixafor mobilization (*20*). We first optimized a selection-free, ribonucleoprotein (RNP)–based protocol (*21*) to efficiently edit the *HBG* promoters in CD34$^+$ HSPCs. The use of chemically modified single gRNAs in combination with a transfection enhancer oligonucleotide resulted in the editing of up to 75% of the alleles using the gRNAs targeting the −200 region (fig. S3A). SCD HSPCs were then transfected with RNP complexes containing either the gRNAs targeting the *HBG* promoters or the control *AAVS1* gRNA. Following erythroid differentiation, genome editing efficiency in bulk populations of mature erythroblasts achieved values of ≥80% in cells transfected with −197, −196, −195, and −115 gRNAs (Fig. 2A and fig. S3B). Editing frequency with the −158 gRNA was variable because of the presence of the C>T SNP at that position in a fraction of the SCD donors (Fig. 2A and fig. S3B). Genome editing efficiency was similar between the *HBG2* and *HBG1* promoters, except for samples harboring the −158 SNP and treated with the −158 gRNA (fig. S3B). Of note, the deletion of the 4.9-kb intervening region between *HBG2* and *HBG1* promoters was not detected in any of the edited primary samples (fig. S3C). This discrepancy between deletion efficiency in HUDEP-2 and HSPCs was also observed in previous studies targeting the −115 region (*19*, *22*) and might be ascribed to a higher expression of the CRISPR-Cas9

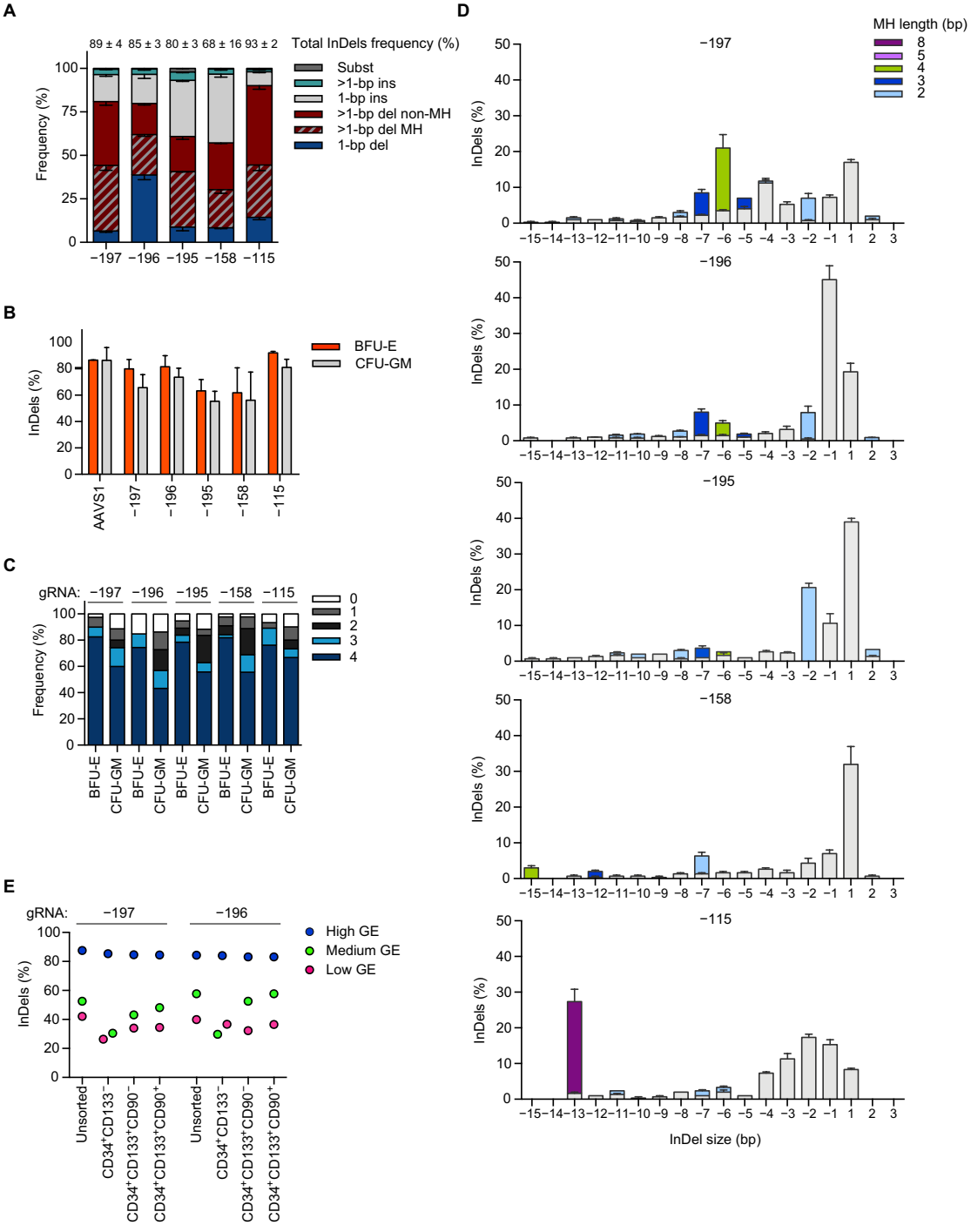

Fig. 2. Efficient editing of *HBG* promoters in HSPCs. (**A**) Deep sequencing analysis of genome editing events in mature erythroblasts derived from adult SCD and CB healthy donor HSPCs. The InDel profile was unchanged between SCD and healthy donor cells. Frequencies of substitutions (subst), insertions (ins), and deletions (del) are shown as percentages of total InDels. The proportion of >1-bp deletions associated or not with MH motifs is indicated. The frequency of >1-bp deletions associated with MH motifs was significantly lower for the −196 gRNA compared to the −197 ($P \leq 0.01$) and −195 ($P \leq 0.001$) gRNAs. Data are expressed as means ± SEM ($n = 3$ to 4, two to three donors). (**B**) Genome editing efficiency in BFU-E and CFU-GM progenitors derived from edited SCD HSPCs as evaluated by TIDE. Data are expressed as means ± SEM ($n = 2$ to 5, two SCD donors). (**C**) Genome editing in single BFU-E and CFU-GM colonies derived from SCD HSPCs as evaluated by TIDE. We plotted the number of edited *HBG* promoters. In the −158 sample, the donor did not harbor the −158 SNP. (**D**) InDel profiles generated by each gRNA as analyzed by deep sequencing. The length of MH motifs associated with specific InDels is indicated. Data are expressed as means ± SEM ($n = 3$ to 4, two to three donors). (**E**) Genome editing efficiency in subpopulations of −197- and −196-edited CB-derived HSPCs. Cells were FACS-sorted based on the expression of CD34, CD133, and CD90, and genome editing efficiency was determined in committed ($CD34^+CD133^-$), early ($CD34^+CD133^+CD90^-$), and primitive ($CD34^+CD133^+CD90^+$) progenitors. We plotted the data of three independent experiments starting from unsorted HSPCs with low, medium, and high genome editing efficiency (three donors).

system in HUDEP-2 cells [transfected with plasmids and FACS (fluorescence-activated cell sorting)–sorted on the basis of Cas9-GFP expression] that favors the simultaneous cleavage of the *HBG* promoters (*23*). However, we cannot exclude that transformed cell lines might be more prone to illegitimate repair and can cope easily with large deletions.

Control and edited SCD HSPCs were plated in clonogenic cultures [colony-forming cell (CFC) assay], allowing the growth of erythroid [burst-forming unit–erythroid (BFU-E)] and granulomonocytic [colony-forming unit–granulomonocytic (CFU-GM)] progenitors. Genome editing efficiency was comparable in pools of BFU-Es and CFU-GMs that showed a similar InDel profile (Fig. 2B and fig. S3D). Clonal analysis of single CFCs revealed that >85% of hematopoietic progenitors were edited at the target sites, with ~86 and ~67% of BFU-Es and CFU-GMs, respectively, displaying ≥3 edited *HBG* promoters (Fig. 2C). Transfection with the full RNP complex reduced the number of hematopoietic progenitors by 10 to 50% compared to transfection of Cas9 protein alone (fig. S3E).

Previous reports have suggested that HSCs, the target of therapeutic genome editing, are preferentially edited via the NHEJ mechanism (*24*, *25*). On the contrary, MMEJ repair pathway, which takes place through annealing of short stretches of identical sequence flanking the double-strand break (DSB), may be less active (*24*, *25*). Therefore, for each gRNA, we evaluated the frequency of mutations with or without MH motifs as a proxy for the relative contribution of MMEJ- and NHEJ-mediated events. In HSPC-derived erythroid bulk populations, among the editing events, deletions were predominant, and a variable fraction of them (30 to 50%) were associated with the presence of MH motifs in the target sequence (Fig. 2A). In particular, MMEJ events at the LRF-binding site can be likely caused by the presence of two stretches of four cytidines (Fig. 1A and table S1). Among the total InDels, the frequency of events associated with MH motifs was significantly higher for the −197 (38 ± 3%) and −195 (32 ± 1%) gRNAs than for the −196 gRNAs (23 ± 1%). The gRNAs targeting the LRF-binding site induced distinct InDel profiles: −196- and −195-edited cells harbored mainly 1-bp insertions and 1- to 2-bp deletions, while the −197 gRNAs generated the largest fraction of >2-bp deletion events, of which ~45% were associated with MH motifs (Fig. 2D and table S1). Virtually all the editing events generated by the −197, −196, and −195 gRNAs disrupted the LRF-binding site (table S1). Of note, the proportion of nucleotides in the LRF-binding site that were lost as a result of editing was higher in −197 than in −196 and −195 samples (fig. S4). As expected, the −115 gRNA caused disruption of the BCL11A-binding site (*19*). In these samples, 13-bp deletions partially spanning the BCL11A-binding site were associated with an 8-bp MH motif and likely mediated by MMEJ (fig. S4 and table S1) (*19*). Last, the −158 gRNA generated mostly 1-bp insertions and small deletions around the cleavage site (Fig. 2D, fig. S4, and table S1). To evaluate CRISPR-Cas9–mediated genetic modification of the $CD34^+$ cell fraction containing more primitive HSPCs, *HBG* promoter editing was assessed in FACS-isolated HSPC subpopulations (*26*), after transfection of the −197 and −196 gRNAs, associated with high and low frequencies of deletions associated with MH motifs, respectively. Editing frequencies were comparable between primitive $CD34^+/CD133^+/CD90^+$ and early $CD34^+/CD133^+/CD90^-$ progenitors and between $CD34^+/CD133^-$ committed progenitors and unsorted $CD34^+$ cells even in the case of a limited genome editing efficiency, with a similar InDel profile across the different $CD34^+$ cell subpopulations (Fig. 2E and fig. S5). It is noteworthy that deletions potentially generated via MMEJ occurred even in the more primitive, HSC-enriched populations (fig. S5).

γ-Globin reactivation following LRF-binding site disruption leads to correction of the SCD cell phenotype

To evaluate HbF reactivation and correction of the SCD cell phenotype upon *HBG* promoter editing, bulk populations of SCD HSPCs were terminally differentiated into enucleated RBCs. Editing of the *HBG* promoters did not affect erythroid differentiation, as evaluated by flow cytometry and RT-qPCR analysis of stage-specific erythroid markers and RBC enucleation and by morphological analysis (fig. S6, A to C). Editing of the −200 region led to increased levels of γ-globin mRNAs, which accounted for 48 ± 3% of total β-like globin transcripts in cells transfected with the −197 gRNA (Fig. 3A). ε-Globin mRNA levels were not significantly different among *HBG*-edited and control samples (fig. S6D). The proportion of F cells in cells transfected with the −197, −196, and −195 gRNAs was 81 ± 1%, 74 ± 2%, and 74 ± 2%, respectively (Fig. 3B). Analysis of −197- and −196-edited erythroblasts sorted by cytofluorimetry based on the intensity of HbF expression revealed a positive correlation between InDel frequency and extent of γ-globin production, indicating that the efficacy of HbF reactivation likely increases when targeting a higher number of *HBG* promoters per cell (fig. S6, E and F). Editing of the −115 region led to *HBG* derepression and a proportion of 80 ± 2% of F cells, while γ-globin reactivation was less pronounced in the −158 samples (55 ± 5% of F cells; Fig. 3, A and B). It is noteworthy that for the −158 gRNA, *HBG* derepression was still modest in RBCs derived from HSPCs harboring >85% of edited *HBG* promoters (Fig. 3, A and B), suggesting that the −158 region contains a sequence that modestly contributes to inhibition of γ-globin expression in adult cells. This is consistent with the mild increase in HbF known to be associated with the −158 SNPs. However, an alternative hypothesis is that these SNPs generate a DNA motif recognized by a still unknown transcriptional activator; thus, the mechanism of action remains unclear. RP-HPLC showed a significant increase in γ-globin chain expression and a reciprocal reduction in β^S-globin levels in the RBC progeny of −200- and −115-edited HSPCs, with no evidence of imbalance in the α/non–α globin chain synthesis (Fig. 3C). In −197-edited cells, the increase in γ-globin chains and the reduction of β^S-globin levels resulted in an inversion of the β/γ globin ratio. Comparable $^A\gamma$- and $^G\gamma$-globin levels were detected in most of the samples analyzed, consistent with the absence of 4.9-kb deletions. However, in −115-edited cells, HbF was mainly composed of $^A\gamma$-globin (fig. S6G). Unexpectedly, in the −115 samples, the relative frequency of the various editing events was different between *HBG1* and *HBG2* promoters, with 13-bp deletions occurring more frequently in *HBG2* than in *HBG1*, while *HBG1* editing events were mainly smaller deletions (table S2). This difference in the editing of *HBG1* and *HBG2* was unexpected and does not obviously explain the altered $^A\gamma/^G\gamma$ ratio in −115-edited samples. CE-HPLC confirmed that editing of the −200 region produced an Hb profile comparable to asymptomatic heterozygous carriers, with HbF representing up to 47 ± 3% of the total Hb tetramers (−197 samples; Fig. 3D). Total Hb levels were comparable between RBCs derived from *HBG*-edited and control HSPCs (fig. S6H).

To assess the effect of HbF reactivation on the sickling phenotype, we performed an in vitro deoxygenation assay that induces sickling of RBCs under hypoxia. At an oxygen concentration of 0%, ~80% of control SCD RBCs acquired a sickled shape (Fig. 3, E and F). Targeting of the −158 region essentially failed to rescue the SCD

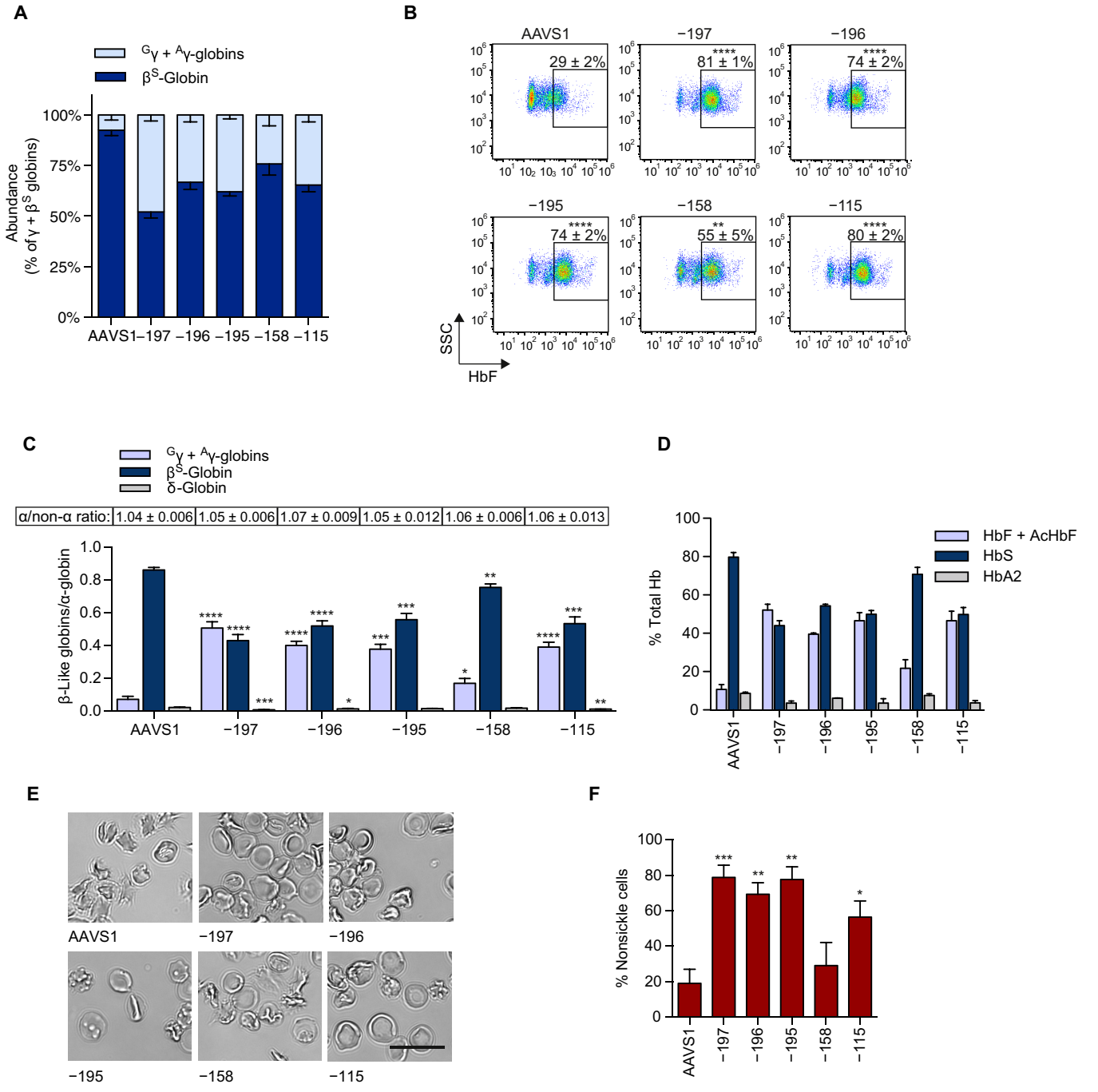

Fig. 3. γ-Globin reactivation and amelioration of the SCD cell phenotype following disruption of LRF-binding site in SCD HSPCs. (**A**) ($^{G}\gamma + {}^{A}\gamma$)- and β^{S}-globin transcript levels detected by RT-qPCR in primary mature erythroblasts. Values are expressed as percentage of ($\gamma + \beta^{S}$)-globin mRNAs after normalization to α-globin. (**B**) Representative flow cytometry plots showing the percentage of HbF^{+} cells in RBC populations derived from control and *HBG*-edited SCD HSPCs. (**C**) RP-HPLC quantification of γ-, β^{S}-, and δ-globin chains. β-Like globin expression was normalized to α-globin. The ratio of α chains to non–α chains was similar between control and *HBG*-edited samples. Data are expressed as means ± SEM. (**D**) Quantification of total HbF (HbF + AcHbF), HbS, and HbA2 by CE-HPLC. We plotted the percentage of each Hb type over the total Hb tetramers. (**E** and **F**) In vitro sickling assay of RBCs derived from edited SCD HSPCs under hypoxic conditions (0% O_2). (E) Representative photomicrographs of RBCs derived from control and *HBG*-edited SCD HSPCs at 0% O_2. Scale bar, 20 μm. (F) Proportion of non-sickled RBCs (0% O_2). (A to F) Data are expressed as means ± SEM ($n = 3$ to 7, two SCD donors). $^{****}P \leq 0.0001$, $^{***}P \leq 0.001$, $^{**}P \leq 0.01$, and $^{*}P \leq 0.05$ versus AAVS1 sample (unpaired *t* test).

phenotype (29 ± 13% of nonsickling RBCs; Fig. 3F). In −115-edited samples, HbF reactivation prevented the sickling of 56 ± 9% of RBCs (Fig. 3F). A marked correction of the SCD phenotype was achieved upon disruption of the LRF-binding site, with 69 ± 6% (−196) to 79 ± 7% (−197) of cells that maintained a biconcave shape under hypoxia (Fig. 3F). Even gRNAs generating predominantly 1- to 2-bp InDels (−195 and −196) induced γ-globin levels that were sufficient to inhibit sickling in a large fraction of RBCs. These results

show that editing of the repressor binding sites in the *HBG* promoters leads to reactivation of HbF sufficient to revert the sickling phenotypes in erythrocytes differentiated from $CD34^+$ HSPCs derived from SCD patients.

Last, in bulk populations of edited SCD erythroblasts, deep sequencing of top-scoring off-targets identified by GUIDE-seq (*27*) in 293T cells (fig. S7A) showed low to undetectable off-target activity at most of the sites. An average InDel frequency of ~20% was observed in cells edited with the −196 gRNA within an intergenic site located on chromosome 12 (OT-196.1) (fig. S7B). This site lies ~15-kb away from the nearest gene and does not map to known regulatory elements involved in hematopoiesis.

Efficient editing of the *HBG* promoters in repopulating HSPCs

We next evaluated editing efficiency in repopulating HSPCs. Mobilized healthy donor HSPCs were transfected with −197, −196, −115, or AAVS1 gRNAs. We achieved an average editing efficiency of 77.3 ± 3.7%, 87.4 ± 4.6%, and 89.6 ± 2.8% for the −197, −196, −115 gRNAs, respectively, as measured in in vitro cultured HSPCs, and BFU-E and CFU-GM pools (input cells). Untreated and edited cells were injected into NSG immunodeficient mice, and 16 weeks after transplantation, we analyzed the engraftment of human hematopoietic cells and editing efficiency. The engraftment of control and *HBG*-edited cells was not statistically different, as analyzed in bone marrow, spleen, and thymus (Fig. 4A), with no skewing toward a particular lineage in any of the samples (fig. S8). Editing efficiency in human cells in the bone marrow and spleen, respectively, was 43.0 ± 9.3% and 33.4 ± 4.0% (−197), 60.3 ± 6.1% and 62.0 ± 1.7% (−196), and 47.6 ± 4.2% and 58.2 ± 3.1% (−115) (Fig. 4B). The −197 gRNA showed a similar InDel profile in the input and in the engrafted human cells, with most of MH motif–associated events occurring at a comparable frequency (Fig. 4C). For the −196 gRNA, events associated to MH motifs were significantly reduced in vivo but were already present at a low frequency in the input populations (Fig. 4C) concordantly with the data obtained in mature erythroblasts in vitro (Fig. 2D). Virtually all editing events disrupt the LRF-binding sites in −197 and −196 samples (Fig. 4C). Last, the frequency of the MH motif–associated 13-bp deletion tended to be lower in the progeny of repopulating HSPCs compared to the input samples, as previously reported (Fig. 4C) (*24*). Together, these results show that the LRF-binding site can be efficiently targeted in engrafting HSPCs.

DISCUSSION

Therapeutic approaches aimed at increasing HbF levels could rely on the down-regulation of nuclear factors involved in γ-globin silencing. However, knockdown of the transcriptional repressor LRF increases HbF expression but delays erythroid differentiation (*28*). Here, we used a CRISPR-Cas9 strategy to disrupt the cis regulatory element involved in LRF-mediated fetal globin silencing and mimic the effect of HPFH mutations. By using three different gRNAs targeting the LRF-binding site, we achieved a robust, virtually pancellular HbF reactivation and a concomitant reduction in β^S-globin levels, recapitulating the phenotype of asymptomatic SCD-HPFH patients (*29*, *30*). Notably, a proportion of HbF >30% in 70% of RBCs has been proposed as the minimal requirement to inhibit HbS polymerization and mitigate the clinical SCD manifestations (*30*). RBCs derived from edited HSPCs displayed HbF levels sufficient to significantly ameliorate the SCD cell phenotype. It is noteworthy that this approach can potentially be applied also to β-thalassemias, where elevated fetal γ-globin levels could compensate for β-globin deficiency.

The development of a selection-free, optimized editing protocol allowed us to obtain a high editing frequency at the LRF-binding site in primary human HSPCs and in HSC-enriched cell populations, which, unexpectedly, showed editing events potentially generated by both NHEJ and MMEJ. However, similarly to the homology-directed repair mechanism (*18*) [used to correct disease-causing mutations (*31*–*33*)], the MMEJ repair pathway occurs in actively dividing cells (*34*). Therefore, we could not exclude that MMEJ might not be efficient in the quiescent repopulating HSCs (*24*, *25*). Xenotransplantation of HSPCs edited using the gRNAs targeting the LRF- or the BCL11A-binding sites demonstrated a high editing efficiency in repopulating HSPCs and no impairment of their multilineage potential. Similarly to recent studies (*24*, *35*), we observed the persistence in vivo of the 13-bp deletion in the −115 region (although at a lower frequency compared to in vitro cultured HSPCs), which is predicted to be mediated by MMEJ. Upon targeting of the *BCL11A* enhancer, Wu and colleagues (*25*) observed a stronger reduction in the frequency of editing events possibly due to MMEJ. In our study, upon targeting of the −200 region, some, but not all, deletions associated with MH motifs and potentially generated via MMEJ were detected at a significantly lower frequency in engrafting HSPCs compared to in vitro cultured HSPCs. Together, these studies suggest that, although at a lower frequency compared to in vitro cultured hematopoietic progenitors, MMEJ can occur in vivo in repopulating HSPCs, in which, however, NHEJ is likely the most active repair pathway. However, as MH motif–associated editing events are "only" computationally predicted to be due to MMEJ, we cannot exclude that a fraction of these events are caused by NHEJ and therefore can occur in repopulating HSPCs.

It is noteworthy that larger deletions typically generated by the −197 edits and associated with an efficient disruption of the LRF-binding sites occur also in vivo. Moreover, even short InDels generated mainly by NHEJ (e.g., −196 gRNA) and detected in repopulating HSPCs are productive in terms of HbF derepression and correction of the SCD cell phenotype. Together, these results show that this strategy can be effective in engrafting HSPCs.

Should the observed editing frequency be confirmed in vivo in patients, this approach would guarantee the efficiency required to achieve clinical benefit in SCD and β-thalassemia. The clinical history of allogeneic HSC transplantation for both diseases suggests that a limited fraction of genetically corrected HSCs would be sufficient to achieve a therapeutic benefit given the in vivo selective survival of corrected RBCs or erythroid precursors (*36*–*41*).

Disrupting either the LRF- or the BCL11A-binding site in the *HBG* promoters induced significant HbF production. Given the independent role of LRF and BCL11A in γ-globin repression (*28*), combined strategies aimed at evicting simultaneously both repressors from the γ-globin promoters could have an additive effect on HbF reactivation. Albeit a Cas9-nuclease–based strategy targeting both the −115 and −200 regions would probably trigger the deletion of the −115-to-200 intervening sequence [that would be detrimental for promoter activity; (*42*)], this study paves the way for the use of novel DSB-free editing strategies [e.g., base editing (*43*)] to simultaneously disrupt both LRF and BCL11A repressor binding sites in the γ-globin promoters.

Overall, our study provides proof of concept for a novel approach to treat SCD by targeting a repressor binding site in the γ-globin

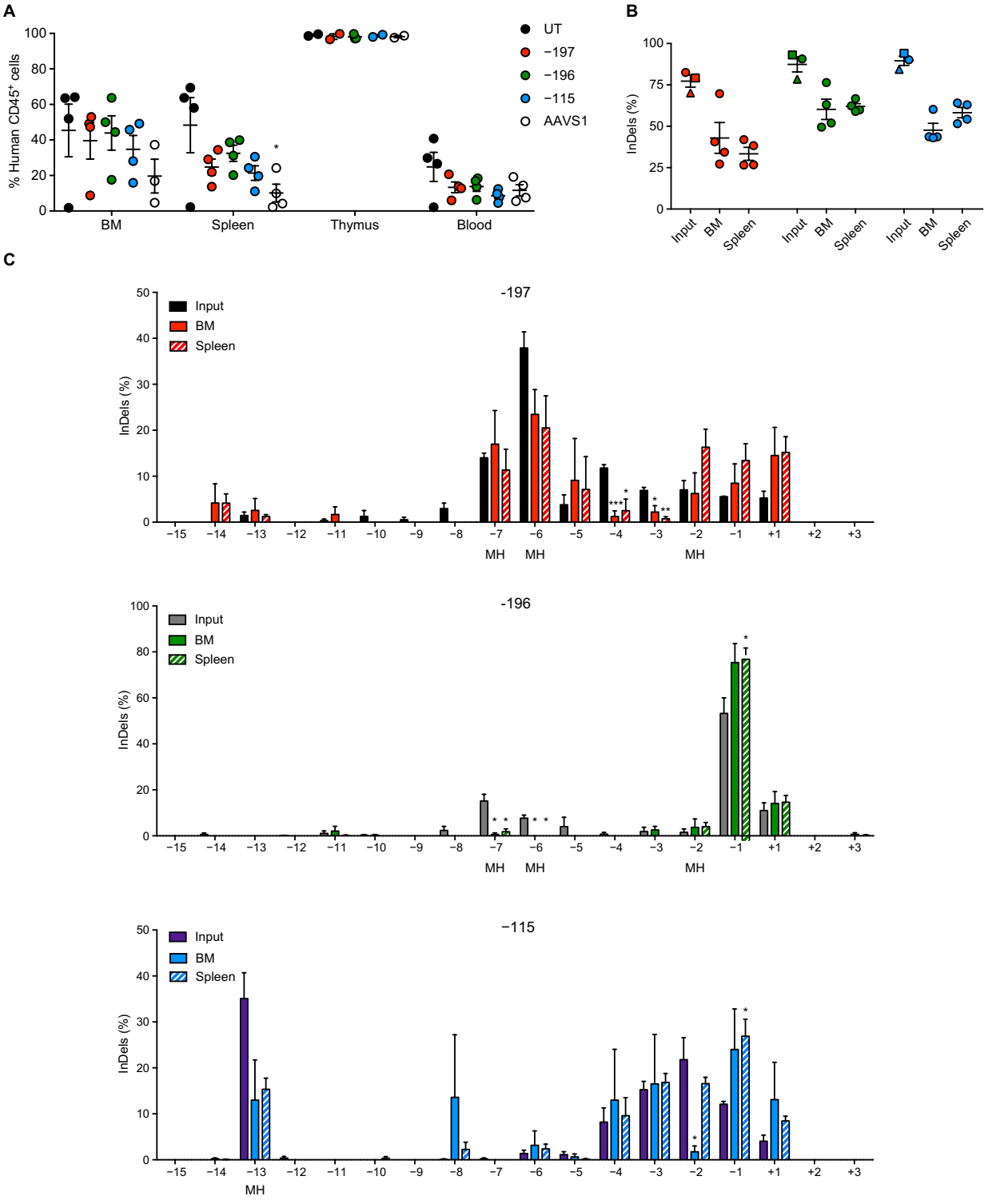

Fig. 4. Editing efficiency in repopulating HSPCs. (**A**) Engraftment of human cells in NSG mice transplanted with untreated (UT) and edited mobilized healthy donor CD34$^+$ cells ($n = 4$ mice for each group) 16 weeks after transplantation. Engraftment is represented as percentage of human CD45$^+$ cells in the total murine and human CD45$^+$ cell population, in bone marrow (BM), spleen, thymus, and blood. Values shown are means ± SEM; *$P \leq 0.05$ versus untreated [one-way analysis of variance (ANOVA)]. (**B**) Editing efficiency in the bone marrow– and spleen-derived human CD45$^+$ progeny of repopulating HSPCs, as evaluated by Sanger sequencing and TIDE analysis. The proportion of edited alleles in the input HSPC populations (○: HSPCs cultured for 6 days in "HSPC medium"; □: BFU-E; △: CFU-GM) is indicated (input). Values shown are means ± SEM. Each data point represents an individual mouse. (**C**) Genome editing efficiency in the input populations and in bone marrow– and spleen-derived human CD45$^+$ populations edited with the −197, −196, or −115 gRNAs, as evaluated by Sanger sequencing and TIDE analysis. The main events associated with MH-motifs are indicated. Values shown are means ± SEM ($n = 4$ mice per group). ***$P \leq 0.001$, **$P \leq 0.01$, and *$P \leq 0.05$ versus input (unpaired t test).

promoters to induce derepression of fetal Hb and a concomitant decrease in HbS synthesis. The same strategy could be beneficial also in the case of β-thalassemia, potentially providing a more economical gene therapy approach compared to the use of LV vectors to deliver a functional β-globin gene. LV manufacturing is complex and very expensive (*44*). Our genome editing approach requires the delivery of RNA/protein reagents that might be less expensive than LV production and thus would allow the broader use of gene therapy for β-hemoglobinopathies.

Clinical translation of this genome editing approach requires the development of nontoxic large-scale transfection protocols based on clinical-grade reagents and demonstration of precise editing in a number of HSPCs at least comparable to the efficacious doses predicted by allogeneic transplantation data (i.e., 2×10^6 to 3×10^6 HSPCs/kg).

MATERIALS AND METHODS

gRNA design and production

We used CRISPOR (*45*) to design gRNAs targeting the −200 and −158 regions of the *HBG* promoters (Table 1). For gRNA expression in erythroid cell lines, oligonucleotide duplexes containing the gRNA protospacers were ligated into Bbs I–digested MA128 plasmid (provided by M. Amendola, Genethon, France). For RNP delivery to HSPCs, we used chemically modified synthetic single gRNAs harboring 2′-*O*-methyl analogs and 3′-phosphorothioate nonhydrolyzable linkages at the first three 5′ and 3′ nucleotides (Synthego) at a concentration of 180 μM. Two-part cr:tracrRNA gRNAs were composed of a tracrRNA (IDT) and a custom crRNA (IDT) assembled in equimolar concentrations to produce a 180 μM duplex (Table 1).

Cell line culture

K562 were maintained in RPMI 1640 (Lonza) containing glutamine and supplemented with 10% fetal bovine serum (Lonza), Hepes (Life Technologies), sodium pyruvate (Life Technologies), and penicillin and streptomycin (Life Technologies). HUDEP-2 cells (*46*) were cultured and differentiated, as previously described (*47*). Flow cytometric analysis of CD36, CD71, and GYPA surface markers and a standard May-Grünwald Giemsa staining were performed to monitor erythroid differentiation.

Cell line transfection

K562 and HUDEP-2 cells were transfected with 4 μg of a Cas9-GFP–expressing plasmid (pMJ920, Addgene) and 0.8 μg (K562) and 1.6 μg (HUDEP-2) of gRNA-containing plasmid. We used AMAXA Cell Line Nucleofector Kit V (VCA-1003) and U-16 and L-29 programs (Nucleofector II) for K562 and HUDEP-2, respectively. GFP^+ HUDEP-2 cells were sorted using SH800 Cell Sorter (Sony Biotechnology).

HSPC purification and culture

We obtained human cord blood (CB) $CD34^+$ HSPCs from healthy donors. CB samples eligible for research purposes were obtained because of a convention with the CB bank of Saint Louis Hospital (Paris, France). Human adult SCD $CD34^+$ HSPCs were isolated from Plerixafor mobilized SCD patients (NCT 02212535 clinical trial, Necker Hospital, Paris, France). We obtained granulocyte colony-stimulating factor (G-CSF)–mobilized adult HSPCs from healthy donors. Written informed consent was obtained from all adult subjects. All experiments were performed in accordance with the Declaration of Helsinki. The study was approved by the regional investigational review board (reference: DC 2014-2272, CPP Ile-de-France II "Hôpital Necker-Enfants malades"). HSPCs were purified by immunomagnetic selection with AutoMACS (Miltenyi Biotec) after immunostaining with the CD34 MicroBead Kit (Miltenyi Biotec).

Forty-eight hours before transfection, $CD34^+$ cells (10^6 cells/ml) were thawed and cultured in the "HSPC medium" containing StemSpan (STEMCELL Technologies) supplemented with penicillin/streptomycin (Gibco), 250 nM StemRegenin1 (STEMCELL Technologies), and the following recombinant human cytokines (PeproTech): stem cell

Table 1. gRNA target sequences. Protospacer adjacent motifs (PAMs) are highlighted in bold.

gRNA	Target sequence (5′ to 3′)	Position (hg19)	Strand
AAVS1	GGGGCCACTAGGGACAGGAT**TGG**	chr19: 55627120–55627139	−
−197	ATTGAGATAGTGTGGGGAAG**GGG**	chr11: 5271268–5271287 (*HBG1*) chr11: 5276192–5276211 (*HBG2*)	+
−196	CATTGAGATAGTGTGGGGAA**GGG**	chr11: 5271267–5271286 (*HBG1*) chr11: 5276191–5276210 (*HBG2*)	+
−195	GCATTGAGATAGTGTGGGGA**AGG**	chr11: 5271266–5271285 (*HBG1*) chr11: 5276190–5276209 (*HBG2*)	+
−158	TATCTGTCTGAAACGGTCCC**TGG**	chr11: 5271243–5271262 (*HBG1*) chr11: 5276167–5276186 (*HBG2*)	−
−152	CCATGGGTGGAGTTTAGCCA**GGG**	chr11: 5271223–5271242 (*HBG1*) chr11: 5276147–5276166 (*HBG2*)	+
−151	CCCATGGGTGGAGTTTAGCC**AGG**	chr11: 5271222–5271241 (*HBG1*) chr11: 5276146–5276165 (*HBG2*)	+
−115	CTTGTCAAGGCTATTGGTCA**AGG**	chr11: 5271186–5271205 (*HBG1*) chr11: 5276110–5276129 (*HBG2*)	+

factor (SCF) (300 ng/ml), Flt-3L (300 ng/ml), thrombopoietin (TPO) (100 ng/ml), and interleukin-3 (IL-3) (60 ng/ml).

HSPC transfection

gRNAs were assembled at room temperature with a 90 μM Cas9-GFP protein (provided by De Cian) in RNP complexes using a ratio of 2:1 (gRNA:Cas9). Human $CD34^+$ cells (1×10^6 to 2×10^6) were transfected with RNP particles using the P3 Primary Cell 4D-Nucleofector X Kit S or L (Lonza), respectively, and the AMAXA 4D CA137 program (Lonza) together with 90 μM transfection enhancer (IDT), unless otherwise stated.

HSPC differentiation

Transfected human HSPCs were differentiated into mature RBCs using a three-step protocol (*48*). From day 0 to day 6, cells were grown in a basal erythroid medium supplemented with the following recombinant human cytokines: SCF (100 ng/ml; PeproTech), IL-3 (5 ng/ml; PeproTech), EPO Eprex (3 IU/ml; Janssen-Cilag), and 10^{-6} M hydrocortisone (Sigma). From day 6 to day 9, cells were cultured onto a layer of murine stromal MS-5 cells in a basal erythroid medium supplemented with EPO Eprex (3 IU/ml). Last, from day 9 to day 19, cells were cultured on a layer of MS-5 cells in a basal erythroid medium without cytokines. Erythroid differentiation was monitored by May Grünwald-Giemsa staining; flow cytometric analysis of CD36, CD71, and GYPA erythroid surface markers; and DRAQ5 staining of nucleated cells.

FACS sorting of HSPC populations

Healthy donor CB-derived $CD34^+$ HSPCs (10^6) were transfected as described above and plated at a concentration of 500,000/ml in StemSpan (STEMCELL Technologies) supplemented with penicillin/streptomycin (Gibco), 250 nM StemRegenin1 (STEMCELL Technologies), and the following recombinant human cytokines (PeproTech): SCF (300 ng/ml), Flt-3L (300 ng/ml), TPO (100 ng/ml), and IL-3 (60 ng/ml). Eighteen hours after transfection, cells were stained with antibodies recognizing CD34 [CD34 phycoerythrin (PE)–Cy7, 348811; BD Pharmingen], CD133 (CD133 PE, 130-113-748, Miltenyi Biotec), and CD90 (CD90 PE-Cy5, 348811, BD Pharmingen). Cells were sorted using FACSAria II (BD Biosciences). Sorted and unsorted populations were cultured at a concentration of 5×10^5/ml in a cytokine-enriched medium (described above) for 4 days before collection for DNA extraction.

Table 2. Primer used to detect InDel events. F, forward primer; R, reverse primer.

Amplified region	F/R	Sequence (5′ to 3′)
HBG1 + *HBG2* promoters	F	AAAAACGGCTGACAAAAGAAGTCCTGGTAT
	R	ATAACCTCAGACGTTCCAGAAGCGAGTGTG
HBG1 promoter	F	TACTGCGCTGAAACTGTGGC
	R	GGCGTCTGGACTAGGAGCTTATTG
HBG2 promoter	F	GCACTGAAACTGTTGCTTTATAGGAT
	R	GGCGTCTGGACTAGGAGCTTATTG
AAVS1	F	CAGCACCAGGATCAGTGAAA
	R	CTATGTCCACTTCAGGACAGCA

CFC assay

The number of hematopoietic progenitors was evaluated by clonal CFC assay. HSPCs were plated at a concentration of 1×10^3 cells/ml in a methylcellulose-containing medium (GFH4435, STEMCELL Technologies) under conditions supporting erythroid and granulo-monocytic differentiation. BFU-E and CFU-GM colonies were scored after 14 days. BFU-Es and CFU-GMs were randomly picked and collected as bulk populations (containing at least 25 colonies) or as individual colonies (35 to 45 colonies per sample) to evaluate genome editing efficiency.

Detection of genome editing events

Genome editing was analyzed in HUDEP-2 cells at days 0 and 9 of erythroid differentiation and in CB and adult mobilized HSPC-derived erythroid cells at days 6 and 14 of erythroid differentiation, respectively. Genomic DNA was extracted from control and edited cells using the PureLink Genomic DNA Mini Kit (Life Technologies), Quick-DNA/RNA Miniprep (ZYMO Research), or DNA Extract All Reagents Kit (Thermo Fisher Scientific) following the manufacturer's instructions. To evaluate NHEJ efficiency at gRNA target sites, we performed PCR followed by Sanger sequencing and TIDE analysis (tracking of InDels by decomposition) (*49*) or ICE CRISPR Analysis Tool (Synthego) (Table 2) (*50*).

Digital droplet PCR was performed using EvaGreen mix (Bio-Rad) to quantify the frequency of the 4.9-kb deletion. Short (~1 min) elongation time allowed the PCR amplification of the genomic region harboring the deletion. Control primers annealing to a genomic region on the same chromosome (chr 11) were used as DNA loading control (Table 3).

Deep sequencing of on- and off-target sites

Following PCR amplification of the target sequences with the Phusion High-Fidelity polymerase with GC Buffer (New England BioLabs), amplicons were purified using Ampure XP beads (Beckman Coulter). Illumina-compatible barcoded DNA amplicon libraries were prepared using the TruSeq DNA PCR-Free kit (Illumina). PCR amplification was then performed using 1 ng of double-stranded ligation product and Kapa Taq polymerase reagents (KAPA HiFi HotStart ReadyMix PCR Kit, Kapa Biosystems). After a purification step using Ampure XP beads (Beckman Coulter), libraries were pooled and sequenced using Illumina HiSeq2500 (paired-end sequencing 130 × 130 bases) (Table 4).

For the on-target sites, read pairs were assembled using FLASH. We used a custom python tool suite to count and characterize InDels that were classified in different types: 1-bp deletions, >1-bp deletions non-MH (not associated with MH motifs), >1-bp deletions MH (associated with MH motifs), 1-bp insertions, and >1-bp insertions and substitutions. A tunable window around the cleavage site

Table 3. Primers used for digital droplet PCR.

Amplified region	F/R	Sequence (5′ to 3′)
HBG1-HBG2 intervening region	F	GTTTTAAAACAACAAAAATGAGGGAAAGA
	R	GTTGCTTTATAGGATTTTTCACTACAC
Chr11 control region	F	CCCTTCCGAGAGGATTTAGG
	R	AGTCGGGATCTGAACAATGG

(typically of 10 bp) was defined to minimize false-positive InDels, and comparison between treated and control samples was used to call InDels due to treatment versus sequencing errors. For the off-target sites, targeted deep sequencing data were analyzed using CRISPRESSO (*51*).

Genome-wide, unbiased identification of DSBs enabled by sequencing

Human embryonic kidney (HEK) 293T/17 cells (2.5×10^5) were transfected with 500 ng of a SpCas9-expressing plasmid, together with 250 ng of each single-guide RNA–coding plasmid or an empty pUC19 vector (background control), 10 pmol of the bait dsODN (designed according to the original GUIDE-seq protocol), and 50 ng of a pEGFP-IRES-Puro plasmid, expressing both enhanced GFP (EGFP) and the puromycin resistance genes. One day after transfection, cells were replated and selected with puromycin (1 μg/ml) for 48 hours to enrich for transfected cells. Cells were then collected, and genomic DNA was extracted using the DNeasy Blood and Tissue Kit (Qiagen) and sheared to an average length of 500 bp with the Bioruptor Pico Sonication System (Diagenode). Library preparation was performed using the original adapters and primers according to previous work (*27*). Libraries were sequenced with a MiSeq sequencing system (Illumina) using an Illumina MiSeq Reagent kit V2-300 cycles (2 × 150-bp paired-end). Raw sequencing data (FASTQ files) were analyzed using the GUIDE-seq computational pipeline (*52*). Identified sites were considered bona fide off-targets if a maximum of seven mismatches against the on-target were present and if they were absent in the background control. The GUIDE-seq datasets are available in the BioProject repository under the accession number PRJNA531587.

Table 4. Primers used for deep sequencing.

Amplified region	F/R	Sequence (5′ to 3′)
HBG promoters	F	GGAATGACTGAATCGGAACAAGG
	R	CTGGCCTCACTGGATACTCT
OT −197.1	F	GTGGGTTATAGAAAGGGCAAGCTG
	R	CCTTCCACTCAGATCTTGCCC
OT −197.2	F	CATCTAAGAGATTGGCAAAAATTATAGAGTCCCAAC
	R	GTAATGTGATTGCTGGGTTGAGCC
OT −197.3	F	CTTCTCAAAAGAGCTAGGTGGCTG
	R	GGGCCAGTACTTCCCTCTTTTTAG
OT −197.4	F	GATAGCACTGGCAACCTGTTTCTG
	R	CTTCACTGTTTTGAGCCTCAGTTTCATTCC
OT −197.5	F	CCTCTTCTCTCCTCCCCTAAC
	R	CCTGCTGTGTTCTAGGCTCTAAG
OT −196.1	F	GTGGGTTATAGAAAGGGCAAGCTG
	R	CCTTCCACTCAGATCTTGCCC
OT −196.2	F	GCCGGGTTAAGGGCGTAGAA
	R	CCCCTCAAACCCACTCTTAAAACC
OT −196.3	F	ATCACTTAAACAAGGATGCTCACCTCAGGTTC
	R	CGGTCCAACCTGGAAATCTCTG
OT −196.4	F	CCCCTTTCATTTACTAACCAGGCATACC
	R	GAGGGGCTTTTACTGGGCAATTG
OT −196.6	F	GTTATGGACTGTAGCAGGACAAGC
	R	GTTGTGAGCCCTTAAAAGGCACAG
OT −195.1	F	ACAAACCATTGTGTGGGACTTTGGAGAC
	R	CTATGCCATGTACTCTCCCTGAC
OT −195.2	F	CATGCCATGAAGGAAAATAAAGCAAGGTAAGAAG
	R	CTAATACATTTCCTTACTTCATTCACGTCACTGC
OT −115.1	F	ATTGGGGGAGACAGACCCATG
	R	CATTTTTATCCAGCTTGGCAGGGG

RT-qPCR analysis of globin and erythroid markers

Total RNA was extracted from differentiated HUDEP-2 (day 9) and primary mature SCD erythroblasts (day 13) using an RNeasy Micro kit (Qiagen), following the manufacturer's instructions. Mature transcripts were reverse-transcribed using SuperScript First-Strand Synthesis System for RT-qPCR (Invitrogen) with oligo(dT) primers. RT-qPCR was performed using an iTaq Universal SYBR Green master mix (Bio-Rad) and a Viia7 Real-Time PCR system (Thermo Fisher Scientific) (Table 5).

RP-HPLC analysis of globin chains

RP-HPLC analysis was performed using a NexeraX2 SIL-30AC chromatograph and the LC Solution software (Shimadzu). Globin chains were separated by HPLC using a 250 mm × 4.6 mm, 3.6-μm Aeris Widepore column (Phenomenex). Samples were eluted with a gradient mixture of solution A (water/acetonitrile/trifluoroacetic acid, 95:5:0.1) and solution B (water/acetonitrile/trifluoroacetic acid, 5:95:0.1). The absorbance was measured at 220 nm.

Table 5. Primer sequences used for RT-qPCR.

Amplified region	F/R	Sequence (5′ to 3′)
HBA	F	CGGTCAACTTCAAGCTCCTAA
	R	ACAGAAGCCAGGAACTTGTC
HBB	F	GCAAGGTGAACGTGGATGAAGT
	R	TAACAGCATCAGGAGTGGACAGA
HBG1 + *HBG2*	F	CCTGTCCTCTGCCTCTGCC
	R	GGATTGCCAAAACGGTCAC
HBD	F	CAAGGGCACTTTTTCTCAG
	R	AATTCCTTGCCAAAGTTGC
HBE	F	CTTTGGAAACCTGTCGTC
	R	CTTGCCAAAGTGAGTAGC
GATA1	F	GACAGGACAGGCCACTACCTATG
	R	AGTACCTGCCCGTTTACTGACAA
ALAS2	F	CAGCGCAATGTCAAGCAC
	R	TAGATGCCATGCTTGGAGAG
BAND3	F	ACCTCTCTCACCTCACCTTCTG
	R	AACCTGTCTAGCAGTTGGTTGG
GAPDH	F	GAAGGTGAAGGTCGGAGT
	R	GAAGATGGTGATGGGATTTC

CE-HPLC analysis of Hb tetramers

CE-HPLC analysis was performed using a NexeraX2 SIL-30 AC chromatograph and the LC Solution software (Shimadzu). Hb tetramers were separated by HPLC using two cation-exchange columns (PolyCAT A, PolyLC, Columbia, MD). Samples were eluted with a gradient mixture of solution A [20 mM Bis-Tris and 2 mM KCN (pH 6.5)] and solution B [20 mM Bis-Tris, 2 mM KCN, and 250 mM NaCl (pH 6.8)]. The absorbance was measured at 415 nm. The calculation of total Hb levels was performed by integration of the areas under the Hb peaks followed by comparison with a standard Hb control (Lyphochek Hemoglobin A2 Control, Bio-Rad).

Flow cytometric analyses

Differentiated HUDEP-2 cells were fixed and permeabilized using BD Cytofix/Cytoperm solution (BD Pharmingen) and stained with an antibody recognizing HbF [an allophycocyanin (APC)–conjugated anti-HbF antibody, MHF05, Life Technologies or a fluorescein isothiocyanate (FITC)–conjugated anti-HbF antibody, 552829, BD Pharmingen]. HSPC-derived RBCs or erythroblasts were fixed in cold 0.05% glutaraldehyde and permeabilized using 0.1% Triton X-100. After incubation with Fcr Blocking Reagent (Miltenyi Biotec), cells were stained with an FITC-conjugated anti-HbF antibody (552829, BD Pharmingen).

Flow cytometric analysis of CD36, CD71, and GYPA erythroid surface markers was performed using a V450-conjugated anti-CD36 antibody (561535, BD Horizon), an FITC-conjugated anti-CD71 antibody (555536, BD Pharmingen), and a PE-Cy7–conjugated anti-GYPA antibody (563666, BD Pharmingen). We used the nuclear dye DRAQ5 (eBioscience) to evaluate the proportion of enucleated RBCs.

To determine genome editing efficiency in erythroid subpopulations, cells were labeled with a PE-Cy7–conjugated anti-GYPA antibody (563666, BD Pharmingen) and an FITC-conjugated anti-HbF antibody (552829, BD Pharmingen), as described above. $GYPA^+$ cells were sorted on the basis of HbF expression using FACSAria II (BD Biosciences).

Flow cytometry analyses were performed using Fortessa X20 (BD Biosciences) or Gallios (Beckman Coulter) flow cytometers. Data were analyzed using the Kaluza software (Beckman Coulter) or the FlowJo software (BD Biosciences).

ChIP assay

ChIP experiments to detect H3K27Ac were performed as previously described (*53*). After 5 days of differentiation, −197 and AAVS1 HUDEP-2 bulk populations were collected for ChIP assays. Briefly, chromatin was cross-linked for 10 min at room temperature with 1% formaldehyde-containing medium. Nuclear extracts were sonicated using the Bioruptor Pico Sonication System (Diagenode). Chromatin obtained from 2×10^6 cells was immunoprecipitated at 4°C overnight using an antibody (1 μg per 10^6 cells) against H3K27Ac (ab4729, Abcam) or a control immunoglobulin G (sc-2025, Santa Cruz Biotechnology). Chromatin cross-linking was reversed at 65°C for at least 4 hours, and DNA was purified using the QIAquick PCR purification kit (Qiagen). We used quantitative SYBR Green PCR (Applied Biosystems) and the Viia7 Real-Time PCR System (Thermo Fisher Scientific) to evaluate H3K27Ac enrichment at different genomic loci (Table 6). ChIP experiments to detect LRF were performed as previously described (*11*) in −197- and AAVS1-edited K562 bulk populations (Table 7).

Table 6. Primers used for ChIP-qPCR (H3K27Ac).

Amplified region	F/R	Sequence (5′ to 3′)
HBB	F	TGCTCCTGGGAGTAGATTGG
	R	TGGTATGGGGCCAAGAGATA
HBG	F	ACAAGCCTGTGGGGCAAGGTG
	R	GCCAGGCACAGGGTCCTTCC

Sickling assay

HSPC-derived SCD RBCs were exposed to an oxygen-deprived atmosphere (0% O_2), and the time course of sickling was monitored in real time by video microscopy, capturing images every 20 min for at least 80 min using an AxioObserver Z1 microscope (Zeiss) and a 40× objective. Images of the same fields were taken throughout all stages and processed with ImageJ to determine the percentage of nonsickled RBCs per field of acquisition in the total RBC population. Cells (~300 to 3300) were counted per condition (1500 cells on average).

NSG mouse transplantation

Nonobese diabetic severe combined immunodeficiency gamma (NSG) mice (NOD.CgPrkdcscid Il2rgtm1Wj/SzJ, Charles River Laboratories, St Germain sur l'Arbresle, France) were housed in a specific pathogen–free facility. Mice at 6 to 8 weeks of age were conditioned with busulfan (Sigma, St. Louis, MO, USA) injected intraperitoneally (25 mg/kg body weight/day) 24, 48, and 72 hours before transplantation. Control or edited mobilized healthy donor $CD34^+$ cells (10^6 cells per mouse) were transplanted into NSG mice via retro-orbital sinus injection. Neomycin and acid water were added in the water bottle. At 16 weeks after transplantation, NSG recipients were sacrificed. Cells were harvested from femur bone marrow, thymus, and spleen; stained with antibodies against murine or human surface markers [murine CD45, BD Biosciences, Franklin Lakes, NJ, USA; human CD45, Miltenyi Biotec, Bergisch Gladbach, Germany; human CD3, Miltenyi Biotec, Bergisch Gladbach, Germany; human CD14, BD Biosciences, Franklin Lakes, NJ, USA; human CD15, Beckman Coulter, Brea, CA, USA; human CD19, Sony Biotechnologies, San Jose, CA, USA; human CD235a (CD235a-APC), BD Pharmingen]; and analyzed by flow cytometry using a Gallios analyzer and the Kaluza software (Beckman Coulter, Brea, CA, USA). All experiments and procedures

Table 7. Primers used for ChIP-qPCR (LRF).

Amplified region	F/R	Sequence (5′ to 3′)
HBG A	F	TCAATGCAAATATCTGTCTGAAACG
	R	CAAGGCTATTGGTCAAGGCAA
HBG B	F	CAAATATCTGTCTGAAACGGTCCC
	R	ACTCTAAGACTATTGGTCAAGTTTGC
KLF1	F	CCCAACCCAGGCAAATTG
	R	GGGCTGGGAGTTGGGTCTT
DEFB122	F	TGTGGCTGGTCCTTGGGCTT
	R	GTGGCTCCTGCCGTGACGAA

were performed in compliance with the French Ministry of Agriculture's regulations on animal experiments and were approved by the regional Animal Care and Use Committee (APAFIS#2101-2015090411495178 v4).

Statistics

Paired *t* tests were performed to compare genome editing efficiencies in erythroid subpopulations sorted based on HbF expression. Unpaired *t* tests were performed for all the other analyses. Statistical analyses were carried out using Prism4 software (GraphPad). We used the Kruskal-Wallis test to compare frequency of deletion generated at each nucleotide by the different gRNAs. The threshold for statistical significance was set to $P < 0.05$.

SUPPLEMENTARY MATERIALS

Supplementary material for this article is available at http://advances.sciencemag.org/cgi/content/full/6/7/eaay9392/DC1

Fig. S1. Genome editing efficiency in erythroid cell lines.
Fig. S2. Erythroid maturation and γ-globin induction in *HBG*-edited HUDEP-2 cells.
Fig. S3. Cas9/gRNA RNP delivery to HSPCs leads to efficient *HBG* promoter editing.
Fig. S4. Deletion frequency at each nucleotide of the *HBG* promoters.
Fig. S5. Genome editing in stem/progenitor populations.
Fig. S6. Erythroid maturation and γ-globin induction in *HBG*-edited erythroid cells derived from SCD HSPCs.
Fig. S7. Off-target analysis.
Fig. S8. Human hematopoietic cell reconstitution in NSG mice transplanted with control and edited HSPCs.
Table S1. Deep sequencing analysis of edited *HBG* promoters in SCD HSPC-derived erythroblasts.
Table S2. Sanger sequencing analysis of −115-edited *HBG1 and HBG2* promoters in SCD HSPC-derived erythroblasts.

View/request a protocol for this paper from *Bio-protocol*.

REFERENCES AND NOTES

1. M. Cavazzana, C. Antoniani, A. Miccio, Gene therapy for β-hemoglobinopathies. *Mol. Ther.* **25**, 1142–1154 (2017).
2. J. Kanter, J. F. Tisdale, J. L. Kwiatkowski, L. Krishnamurti, M. Y. Mapara, M. Schmidt, A. L. Miller, F. J. Pierciey Jr., W. Shi, J.-A. Ribeil, M. C. Walters, A. A. Thompson, Outcomes for initial patient cohorts with up to 33 months of follow-up in the Hgb-206 phase 1 trial, paper presented at the 60th ASH Annual Meeting, San Diego, CA, 1 to 4 December 2018.
3. A. A. Thompson, M. C. Walters, J. Kwiatkowski, J. E. J. Rasko, J. A. Ribeil, S. Hongeng, E. Magrin, G. J. Schiller, E. Payen, M. Semeraro, D. Moshous, F. Lefrere, H. Puy, P. Bourget, A. Magnani, L. Caccavelli, J. S. Diana, F. Suarez, F. Monpoux, V. Brousse, C. Poirot, C. Brouzes, J. F. Meritet, C. Pondarré, Y. Beuzard, S. Chrétien, T. Lefebvre, D. T. Teachey, U. Anurathapan, P. J. Ho, C. von Kalle, M. Kletzel, E. Vichinsky, S. Soni, G. Veres, O. Negre, R. W. Ross, D. Davidson, A. Petrusich, L. Sandler, M. Asmal, O. Hermine, M. de Montalembert, S. Hacein-Bey-Abina, S. Blanche, P. Leboulch, M. Cavazzana, Gene therapy in patients with transfusion-dependent β-Thalassemia. *N. Engl. J. Med.* **378**, 1479–1493 (2018).
4. S. Marktel, S. Scaramuzza, M. P. Cicalese, F. Giglio, S. Galimberti, M. R. Lidonnici, V. Calbi, A. Assanelli, M. E. Bernardo, C. Rossi, A. Calabria, R. Milani, S. Gattillo, F. Benedicenti, G. Spinozzi, A. Aprile, A. Bergami, M. Casiraghi, G. Consiglieri, N. Masera, E. D'Angelo, N. Mirra, R. Origa, I. Tartaglione, S. Perrotta, R. Winter, M. Coppola, G. Viarengo, L. Santoleri, G. Graziadei, M. Gabaldo, M. G. Valsecchi, E. Montini, L. Naldini, M. D. Cappellini, F. Ciceri, A. Aiuti, G. Ferrari, Intrabone hematopoietic stem cell gene therapy for adult and pediatric patients affected by transfusion-dependent β-thalassemia. *Nat. Med.* **25**, 234–241 (2019).
5. J. A. Ribeil, S. Hacein-Bey-Abina, E. Payen, A. Magnani, M. Semeraro, E. Magrin, L. Caccavelli, B. Neven, P. Bourget, W. el Nemer, P. Bartolucci, L. Weber, H. Puy, J. F. Meritet, D. Grevent, Y. Beuzard, S. Chrétien, T. Lefebvre, R. W. Ross, O. Negre, G. Veres, L. Sandler, S. Soni, M. de Montalembert, S. Blanche, P. Leboulch, M. Cavazzana, Gene therapy in a patient with sickle cell disease. *N. Engl. J. Med.* **376**, 848–855 (2017).
6. N. Herbert, E. Magrin, A. Miccio, K. Laurent, N. P. Kim-Anh, L. Joseph, A. Magnani, C. Couzin, W. El Nemer, F. Pirenne, O. Negre, Analysis of RBC properties in patients with SCD treated with LentiGlobin gene therapy, paper presented at the 60th ASH Annual Meeting, San Diego, CA, 1 to 4 December 2018.
7. B. G. Forget, Molecular basis of hereditary persistence of fetal hemoglobin. *Ann. N. Y. Acad. Sci.* **850**, 38–44 (1998).
8. B. Wienert, G. E. Martyn, A. P. W. Funnell, K. G. R. Quinlan, M. Crossley, Wake-up sleepy gene: Reactivating fetal globin for β-hemoglobinopathies. *Trends Genet.* **34**, 927–940 (2018).
9. B. Wienert, A. P. W. Funnell, L. J. Norton, R. C. M. Pearson, L. E. Wilkinson-White, K. Lester, J. Vadolas, M. H. Porteus, J. M. Matthews, K. G. R. Quinlan, M. Crossley, Editing the genome to introduce a beneficial naturally occurring mutation associated with increased fetal globin. *Nat. Commun.* **6**, 7085 (2015).
10. B. Wienert, G. E. Martyn, R. Kurita, Y. Nakamura, K. G. R. Quinlan, M. Crossley, KLF1 drives the expression of fetal hemoglobin in British HPFH. *Blood* **130**, 803–807 (2017).
11. G. E. Martyn, B. Wienert, L. Yang, M. Shah, L. J. Norton, J. Burdach, R. Kurita, Y. Nakamura, R. C. M. Pearson, A. P. W. Funnell, K. G. R. Quinlan, M. Crossley, Natural regulatory mutations elevate the fetal globin gene via disruption of BCL11A or ZBTB7A binding. *Nat. Genet.* **50**, 498–503 (2018).
12. N. Liu, V. V. Hargreaves, Q. Zhu, J. V. Kurland, J. Hong, W. Kim, F. Sher, C. Macias-Trevino, J. M. Rogers, R. Kurita, Y. Nakamura, G. C. Yuan, D. E. Bauer, J. Xu, M. L. Bulyk, S. H. Orkin, Direct promoter repression by BCL11A controls the fetal to adult hemoglobin switch. *Cell* **173**, 430–442.e17 (2018).
13. S. L. Thein, J. S. Wainscoat, M. Sampietro, J. M. Old, D. Cappellini, G. Fiorelli, B. Modell, D. J. Weatherall, Association of thalassaemia intermedia with a beta-globin gene haplotype. *Br. J. Haematol.* **65**, 367–373 (1987).
14. P. J. Ho, G. W. Hall, L. Y. Luo, D. J. Weatherall, S. L. Thein, Beta-thalassaemia intermedia: Is it possible consistently to predict phenotype from genotype? *Br. J. Haematol.* **100**, 70–78 (1998).
15. D. Labie, O. Dunda-Belkhodja, F. Rouabhi, J. Pagnier, A. Ragusa, R. L. Nagel, The −158 site 5′ to the G gamma gene and G gamma expression. *Blood* **66**, 1463–1465 (1985).
16. G. Galarneau, C. D. Palmer, V. G. Sankaran, S. H. Orkin, J. N. Hirschhorn, G. Lettre, Fine-mapping at three loci known to affect fetal hemoglobin levels explains additional genetic variation. *Nat. Genet.* **42**, 1049–1051 (2010).
17. J. G. Gilman, T. H. Huisman, DNA sequence variation associated with elevated fetal G gamma globin production. *Blood* **66**, 783–787 (1985).
18. P. Genovese, G. Schiroli, G. Escobar, T. D. Tomaso, C. Firrito, A. Calabria, D. Moi, R. Mazzieri, C. Bonini, M. C. Holmes, P. D. Gregory, M. van der Burg, B. Gentner, E. Montini, A. Lombardo, L. Naldini, Targeted genome editing in human repopulating haematopoietic stem cells. *Nature* **510**, 235–240 (2014).
19. E. A. Traxler, Y. Yao, Y. D. Wang, K. J. Woodard, R. Kurita, Y. Nakamura, J. R. Hughes, R. C. Hardison, G. A. Blobel, C. Li, M. J. Weiss, A genome-editing strategy to treat β-hemoglobinopathies that recapitulates a mutation associated with a benign genetic condition. *Nat. Med.* **22**, 987–990 (2016).
20. C. Lagresle-Peyrou, F. Lefrère, E. Magrin, J. A. Ribeil, O. Romano, L. Weber, A. Magnani, H. Sadek, C. Plantier, A. Gabrion, B. Ternaux, T. Félix, C. Couzin, A. Stanislas, J. M. Tréluyer, L. Lamhaut, L. Joseph, M. Delville, A. Miccio, I. André-Schmutz, M. Cavazzana, Plerixafor enables safe, rapid, efficient mobilization of hematopoietic stem cells in sickle cell disease patients after exchange transfusion. *Haematologica* **103**, 778–786 (2018).
21. A. Lattanzi, Optimization of CRISPR/Cas9 delivery to human hematopoietic stem and progenitor cells for therapeutic genomic rearrangements. *Mol. Ther.* **27**, 137–150 (2018).
22. C. Li, N. Psatha, P. Sova, S. Gil, H. Wang, J. Kim, C. Kulkarni, C. Valensisi, R. D. Hawkins, G. Stamatoyannopoulos, A. Lieber, Reactivation of γ-globin in adult β-YAC mice after ex vivo and in vivo hematopoietic stem cell genome editing. *Blood* **131**, 2915–2928 (2018).
23. A. Lattanzi, V. Meneghini, G. Pavani, F. Amor, S. Ramadier, T. Felix, C. Antoniani, C. Masson, O. Alibeu, C. Lee, M. H. Porteus, G. Bao, M. Amendola, F. Mavilio, A. Miccio, Optimization of CRISPR/Cas9 delivery to human hematopoietic stem and progenitor cells for therapeutic genomic rearrangements. *Mol. Ther.* **27**, 137–150 (2019).
24. C. T. Lux, S. Pattabhi, M. Berger, C. Nourigat, D. A. Flowers, O. Negre, O. Humbert, J. G. Yang, C. Lee, K. Jacoby, I. Bernstein, H. P. Kiem, A. Scharenberg, D. J. Rawlings, TALEN-mediated gene editing of HBG in human hematopoietic stem cells leads to therapeutic fetal hemoglobin induction. *Mol. Ther. Methods Clin. Dev.* **12**, 175–183 (2019).
25. Y. Wu, J. Zeng, B. P. Roscoe, P. Liu, Q. Yao, C. R. Lazzarotto, K. Clement, M. A. Cole, K. Luk, C. Baricordi, A. H. Shen, C. Ren, E. B. Esrick, J. P. Manis, D. M. Dorfman, D. A. Williams, A. Biffi, C. Brugnara, L. Biasco, C. Brendel, L. Pinello, S. Q. Tsai, S. A. Wolfe, D. E. Bauer, Highly efficient therapeutic gene editing of human hematopoietic stem cells. *Nat. Med.* **25**, 776–783 (2019).
26. G. Schiroli, S. Ferrari, A. Conway, A. Jacob, V. Capo, L. Albano, T. Plati, M. C. Castiello, F. Sanvito, A. R. Gennery, C. Bovolenta, R. Palchaudhuri, D. T. Scadden, M. C. Holmes, A. Villa, G. Sitia, A. Lombardo, P. Genovese, L. Naldini, Preclinical modeling highlights the therapeutic potential of hematopoietic stem cell gene editing for correction of SCID-X1. *Sci. Transl. Med.* **9**, eaan0820 (2017).
27. S. Q. Tsai, Z. Zheng, N. T. Nguyen, M. Liebers, V. V. Topkar, V. Thapar, N. Wyvekens, C. Khayter, A. J. Iafrate, L. P. Le, M. J. Aryee, J. K. Joung, GUIDE-seq enables genome-wide profiling of off-target cleavage by CRISPR-Cas nucleases. *Nat. Biotechnol.* **33**, 187–197 (2015).

28. T. Masuda, X. Wang, M. Maeda, M. C. Canver, F. Sher, A. P. W. Funnell, C. Fisher, M. Suciu, G. E. Martyn, L. J. Norton, C. Zhu, R. Kurita, Y. Nakamura, J. Xu, D. R. Higgs, M. Crossley, D. E. Bauer, S. H. Orkin, P. V. Kharchenko, T. Maeda, Transcription factors LRF and BCL11A independently repress expression of fetal hemoglobin. *Science* **351**, 285–289 (2016).
29. I. Akinsheye, A. Alsultan, N. Solovieff, D. Ngo, C. T. Baldwin, P. Sebastiani, D. H. K. Chui, M. H. Steinberg, Fetal hemoglobin in sickle cell anemia. *Blood* **118**, 19–27 (2011).
30. M. H. Steinberg, D. H. Chui, G. J. Dover, P. Sebastiani, A. Alsultan, Fetal hemoglobin in sickle cell anemia: A glass half full? *Blood* **123**, 481–485 (2014).
31. M. A. DeWitt, W. Magis, N. L. Bray, T. Wang, J. R. Berman, F. Urbinati, S. J. Heo, T. Mitros, D. P. Muñoz, D. Boffelli, D. B. Kohn, M. C. Walters, D. Carroll, D. I. K. Martin, J. E. Corn, Selection-free genome editing of the sickle mutation in human adult hematopoietic stem/progenitor cells. *Sci. Transl. Med.* **8**, 360ra134 (2016).
32. M. D. Hoban, D. Lumaquin, C. Y. Kuo, Z. Romero, J. Long, M. Ho, C. S. Young, M. Mojadidi, S. Fitz-Gibbon, A. R. Cooper, G. R. Lill, F. Urbinati, B. Campo-Fernandez, C. F. Bjurstrom, M. Pellegrini, R. P. Hollis, D. B. Kohn, CRISPR/Cas9-mediated correction of the sickle mutation in human CD34+ cells. *Mol. Ther.* **24**, 1561–1569 (2016).
33. D. P. Dever, R. O. Bak, A. Reinisch, J. Camarena, G. Washington, C. E. Nicolas, M. Pavel-Dinu, N. Saxena, A. B. Wilkens, S. Mantri, N. Uchida, A. Hendel, A. Narla, R. Majeti, K. I. Weinberg, M. H. Porteus, CRISPR/Cas9 β-globin gene targeting in human haematopoietic stem cells. *Nature* **539**, 384–389 (2016).
34. L. N. Truong, Y. Li, L. Z. Shi, P. Y. Hwang, J. He, H. Wang, N. Razavian, M. W. Berns, X. Wu, Microhomology-mediated end joining and homologous recombination share the initial end resection step to repair DNA double-strand breaks in mammalian cells. *Proc. Natl. Acad. Sci. U.S.A.* **110**, 7720–7725 (2013).
35. O. Humbert, S. Radtke, C. Samuelson, R. R. Carrillo, A. M. Perez, S. S. Reddy, C. Lux, S. Pattabhi, L. E. Schefter, O. Negre, C. M. Lee, G. Bao, J. E. Adair, C. W. Peterson, D. J. Rawlings, A. M. Scharenberg, H. P. Kiem, Therapeutically relevant engraftment of a CRISPR-Cas9-edited HSC-enriched population with HbF reactivation in nonhuman primates. *Sci. Transl. Med.* **11**, eaaw3768 (2019).
36. R. S. Franco, Z. Yasin, M. B. Palascak, P. Ciraolo, C. H. Joiner, D. L. Rucknagel, The effect of fetal hemoglobin on the survival characteristics of sickle cells. *Blood* **108**, 1073–1076 (2006).
37. F. Centis, L. Tabellini, G. Lucarelli, O. Buffi, P. Tonucci, B. Persini, M. Annibali, R. Emiliani, A. Iliescu, S. Rapa, R. Rossi, L. Ma, E. Angelucci, S. L. Schrier, The importance of erythroid expansion in determining the extent of apoptosis in erythroid precursors in patients with beta-thalassemia major. *Blood* **96**, 3624–3629 (2000).
38. M. C. Walters, M. Patience, W. Leisenring, Z. R. Rogers, V. M. Aquino, G. R. Buchanan, I. A. Roberts, A. M. Yeager, L. Hsu, T. Adamkiewicz, J. Kurtzberg, E. Vichinsky, B. Storer, R. Storb, K. M. Sullivan; Multicenter Investigation of Bone Marrow Transplantation for Sickle Cell Disease, Stable mixed hematopoietic chimerism after bone marrow transplantation for sickle cell anemia. *Biol. Blood Marrow Transplant.* **7**, 665–673 (2001).
39. A. Miccio, R. Cesari, F. Lotti, C. Rossi, F. Sanvito, M. Ponzoni, S. J. E. Routledge, C. M. Chow, M. N. Antoniou, G. Ferrari, In vivo selection of genetically modified erythroblastic progenitors leads to long-term correction of β-thalassemia. *Proc. Natl. Acad. Sci. U.S.A.* **105**, 10547–10552 (2008).
40. P. M. Altrock, C. Brendel, R. Renella, S. H. Orkin, D. A. Williams, F. Michor, Mathematical modeling of erythrocyte chimerism informs genetic intervention strategies for sickle cell disease. *Am. J. Hematol.* **91**, 931–937 (2016).
41. A. Abraham, M. Hsieh, M. Eapen, C. Fitzhugh, J. Carreras, D. Keesler, G. Guilcher, N. Kamani, M. C. Walters, J. J. Boelens, J. Tisdale, S. Shenoy; National Institutes of Health; Center for International Blood and Marrow Transplant Research, Relationship between mixed donor-recipient chimerism and disease recurrence after hematopoietic cell transplantation for sickle cell disease. *Biol. Blood Marrow Transplant.* **23**, 2178–2183 (2017).
42. G. E. Martyn, K. G. R. Quinlan, M. Crossley, The regulation of human globin promoters by CCAAT box elements and the recruitment of NF-Y. *Biochim. Biophys. Acta* **1860**, 525–536 (2017).
43. A. C. Komor, A. H. Badran, D. R. Liu, Editing the genome without double-stranded DNA breaks. *ACS Chem. Biol.* **13**, 383–388 (2018).
44. S. Coquerelle, M. Ghardallou, S. Rais, P. Taupin, F. Touzot, L. Boquet, S. Blanche, S. Benaouadi, T. Brice, C. Tuchmann-Durand, J. A. Ribeil, E. Magrin, E. Lissillour, L. Rochaix, M. Cavazzana, I. Durand-Zaleski, Innovative curative treatment of beta thalassemia: Cost-efficacy analysis of gene therapy versus allogenic hematopoietic stem-cell transplantation. *Hum. Gene Ther.* **30**, 753–761 (2019).
45. M. Haeussler, K. Schönig, H. Eckert, A. Eschstruth, J. Mianné, J. B. Renaud, S. Schneider-Maunoury, A. Shkumatava, L. Teboul, J. Kent, J. S. Joly, J. P. Concordet, Evaluation of off-target and on-target scoring algorithms and integration into the guide RNA selection tool CRISPOR. *Genome Biol.* **17**, 148 (2016).
46. R. Kurita, N. Suda, K. Sudo, K. Miharada, T. Hiroyama, H. Miyoshi, K. Tani, Y. Nakamura, Establishment of immortalized human erythroid progenitor cell lines able to produce enucleated red blood cells. *PLOS ONE* **8**, e59890 (2013).
47. C. Antoniani, V. Meneghini, A. Lattanzi, T. Felix, O. Romano, E. Magrin, L. Weber, G. Pavani, S. El Hoss, R. Kurita, Y. Nakamura, T. J. Cradick, A. S. Lundberg, M. H. Porteus, M. Amendola, W. El-Nemer, M. Cavazzana, F. Mavilio, A. Miccio, Induction of fetal hemoglobin synthesis by CRISPR/Cas9-mediated editing of the human β-globin locus. *Blood* **131**, 1960–1973 (2018).
48. M. C. Giarratana, L. Kobari, H. Lapillonne, D. Chalmers, L. Kiger, T. Cynober, M. C. Marden, H. Wajcman, L. Douay, Ex vivo generation of fully mature human red blood cells from hematopoietic stem cells. *Nat. Biotechnol.* **23**, 69–74 (2005).
49. E. K. Brinkman, T. Chen, M. Amendola, B. van Steensel, Easy quantitative assessment of genome editing by sequence trace decomposition. *Nucleic Acids Res.* **42**, e168 (2014).
50. T. Hsiau, D. Conant, N. Rossi, T. maures, K. Waite, J. Yang, S. Joshi, R. Kelso, K. Holden, B. L. Enxmann, R. Stoner, Inference of CRISPR edits from Sanger trace data. bioRxiv 251082 [**Preprint**]. 10 August 2019. https://doi.org/10.1101/251082.
51. L. Pinello, M. C. Canver, M. D. Hoban, S. H. Orkin, D. B. Kohn, D. E. Bauer, G. C. Yuan, Analyzing CRISPR genome-editing experiments with CRISPResso. *Nat. Biotechnol.* **34**, 695–697 (2016).
52. S. Q. Tsai, V. V. Topkar, J. K. Joung, M. J. Aryee, Open-source guideseq software for analysis of GUIDE-seq data. *Nat. Biotechnol.* **34**, 483 (2016).
53. O. Romano, C. Peano, G. M. Tagliazucchi, L. Petiti, V. Poletti, F. Cocchiarella, E. Rizzi, M. Severgnini, A. Cavazza, C. Rossi, P. Pagliaro, A. Ambrosi, G. Ferrari, S. Bicciato, G. de Bellis, F. Mavilio, A. Miccio, Transcriptional, epigenetic and retroviral signatures identify regulatory regions involved in hematopoietic lineage commitment. *Sci. Rep.* **6**, 24724 (2016).

Acknowledgments: We thank R. Kurita and Y. Nakamura for contributing the HUDEP-2 cell line, L. Douay for the erythroid differentiation protocol, G. Pavani for the optimization of editing protocol in HSPCs, B. Wienert for providing assistance and protocol for the LRF ChIP, O. Alibeau and C. Bole for the DNA sequencing, E. Brunet for the discussion, and E. Duvernois-Berthet for the script used for InDel characterization. **Funding:** This work was supported by grants from the European Research Council (ERC-2015-AdG, GENEFORCURE), the Agence Nationale de la Recherche (ANR-16-CE18-0004, ANR-11-INBS-0014-TEFOR, ANR-17-CE13-0016-i-MMEJ, and ANR-10-IAHU-01 "Investissements d'avenir" program), the Paris Ile-de-France Region under «DIM Thérapie génique» initiative, the AFM-Telethon (22399 and 22206), and Genopole (CHAIRE JUNIOR FONDAGEN). **Author contributions:** L.W. and G.F. designed and conducted the experiments and wrote the paper. T.F., G.H., A.Ca., C.W., V.M., and A.Ch. designed and conducted the experiments. C.M. analyzed off-target NGS data. A.D.C. provided reagents. F.M., M.A., I.A.-S., A.Ce., W.E.N., J.-P.C., C.G., and M.C. contributed to the design of the experimental strategy. A.M. conceived the study, designed the experiments, and wrote the paper. **Competing interests:** A.M. and L.W. are inventors on a patent application related to this work filed by INSERM (PCT/EP2019/074131, 10 September 2019). The authors declare that they have no other competing interests. **Data and materials availability:** The GUIDE-seq datasets are available in the BioProject repository under the accession number PRJNA531587. The datasets containing deep sequencing of on- and off-target sites are available in the BioProject repository under the accession number PRJNA602385. All data needed to evaluate the conclusions in the paper are present in the paper and/or the Supplementary Materials. Additional data related to this paper may be requested from the authors.

Submitted 30 July 2019
Accepted 25 November 2019
Published 12 February 2020
10.1126/sciadv.aay9392

Citation: L. Weber, G. Frati, T. Felix, G. Hardouin, A. Casini, C. Wollenschlaeger, V. Meneghini, C. Masson, A. De Cian, A. Chalumeau, F. Mavilio, M. Amendola, I. Andre-Schmutz, A. Cereseto, W. El Nemer, J.-P. Concordet, C. Giovannangeli, M. Cavazzana, A. Miccio, Editing a γ-globin repressor binding site restores fetal hemoglobin synthesis and corrects the sickle cell disease phenotype. *Sci. Adv.* **6**, eaay9392 (2020).

ScienceAdvances

Editing a #-globin repressor binding site restores fetal hemoglobin synthesis and corrects the sickle cell disease phenotype

Leslie Weber, Giacomo Frati, Tristan Felix, Giulia Hardouin, Antonio Casini, Clara Wollenschlaeger, Vasco Meneghini, Cecile Masson, Anne De Cian, Anne Chalumeau, Fulvio Mavilio, Mario Amendola, Isabelle Andre-Schmutz, Anna Cereseto, Wassim El Nemer, Jean-Paul Concordet, Carine Giovannangeli, Marina Cavazzana, and Annarita Miccio

Sci. Adv., **6** (7), eaay9392.
DOI: 10.1126/sciadv.aay9392

Science Advances (ISSN 2375-2548) is published by the American Association for the Advancement of Science. 1200 New York Avenue NW, Washington, DC 20005. The title *Science Advances* is a registered trademark of AAAS.